Eur. Phys. J. B **55**, 37–42 (2007)
DOI: 10.1140/epjb/e2007-00039-1

THE EUROPEAN PHYSICAL JOURNAL B

Brillouin-zone mapping of the spin waves in a ferromagnetic bilayer system

W.P. Zhou[a], G.H. Yun[b], and X.X. Liang

Laboratory of solid State Physics, Department of Physics, Inner Mongolia University, Hohhot 010021, Inner Mongolia, P.R. China
CCAST (World Laboratory), P.O. Box 8730, Beijing 100080, P.R. China

Received 1st November 2006 / Received in final form 25 December 2006
Published online 9 February 2007 –

Abstract. The eigenproblems of spin waves in a heterogeneous ferromagnetic bilayer system with periodic boundary conditions are solved using the interface-rescaling approach. Brillouin zone mapping and the eigenmodes of the system are investigated. We find three types of spin waves may exist in the system: the bulk mode, the interface mode, and the perfect confined mode. The fine structure of the energy band in the heterogeneous bilayer system is first given for the whole two-dimensional Brillouin zone. Conditions for the existence of the interface mode are discussed. Finally, we analyze the resonant-confined spin waves in bulk modes and their oscillating behavior.

PACS. 75.30.Ds Spin waves

1 Introduction

Magnetic multilayers have many fascinating properties such as collective features and the giant magnetoresistance effect [1,2]. Many applications utilize these properties, such as magnetic field sensors [3], spin valve read heads for hard drives [4], magnetoresistive random access memory [5], and so on. For faster information access, magnetic recording based on magnetic multilayered media is considered an ideal data storage solution. The advantages of these devices would be non-volatility, increased data processing speed, decreased electric power consumption and increased integration densities [6–9]. Gbits of information can now be accessed in a nanosecond using these devices, however new problems arise. When reading or writing data at Gbits per nanosecond, the magnetic system is excited at GHz rates [10,11] and the generation of spin waves will strongly influence the response of magnetic recording media. Therefore thorough study of spin-wave eigenmodes [12–16] will be helpful to conveniently control these devices.

Puszkarski et al. [17,18] introduced an interface-rescaling approach (IRA). This method can exactly solve the eigenproblems of layered magnetic materials by decomposing the complex systems into independent subsystems. With this method, many authors have investigated different magnetic properties of layered magnetic materials, such as conditions for interface spin waves in a system of ferromagnetic bilayers [19–21], the dispersion relations of spin waves, ferromagnetic resonance spectra and anisotropy in a general system of ferromagnetic bilayers [22–27].

In references [19,20], authors studied extensively the conditions for the existence of interface spin waves (ISW) in various bilayer cubic systems (s.c, b.c.c and f.c.c), composed of two symmetrical, semi-infinite ferromagnetic sublayers, applying Brillouin-zone mapping for the three interface orientations (100), (110), and (111). Recently, we use IRA to exactly solve the eigenproblems of ISW of a (100) biferromagnetic interface and obtain analytically the necessary and sufficient conditions for the existence of ISW in such systems [21]. In reference [27], the authors discussed the interface-localized mode in an ultrathin bilayer system. About ten years ago, we studied the bulk spin waves of a general system of ferromagnetic bilayers only when $k_{||} = 0$, and found the resonant-confined spin waves only in one sublayer [22]. At the same time, we discussed the effect of the transverse spin waves and the uniaxial bulk anisotropy field on the dispersion relations in a general system of ferromagnetic bilayers with the interface exchange coupling constant being greater than zero only when $k_{||} < \pi/2$ [24]. In this paper we shall study the fine structure of the energy band and the eigenmodes of spin waves on the whole two-dimensional (2D) Brillouin zone, discuss conditions for the existence of ISW in two cases of the interface exchange coupling constant being greater and less than zero, and in particular analyze the resonant-confined spin waves in bulk modes and their oscillating behaviors in both sublayers in the same systems as reference [24].

[a] e-mail: wenpingzhou73@yahoo.com.cn
[b] e-mail: ghyun @imu.edu.cn

2 The model and eigenmodes

Consider a simple cubic ferromagnetic bilayer slab consisting of two homogeneous sublayers A and B with the bulk-exchange interactions J_A and J_B, the interface exchange coupling J_{AB}, the spins S_A and S_B, and the numbers of lattice planes N_A and N_B, respectively. For the sake of simplicity, we assume the two ferromagnets still have their periodicity in the lattice planes parallel to the interface. Here we neglect the anisotropy in the bulk, on the interface and on the surfaces, so that the inhomogeneity of the system is assumed to come from the difference between the interface and bulk exchange couplings J_{AB}, J_A and J_B. Under a periodic boundary condition we assume the Heisenberg Hamiltonian consists of two terms accounting for the isotropic nearest-neighbor (NN) exchange interaction and the Zeeman energy of the spins. Hence the Hamiltonian of such system is written as:

$$H = -\sum_{n,m}\sum_{i,j} J(n,i;m,j)\Big\{\frac{1}{2}[S^+(n,i)\cdot S^-(m,j) + S^-(n,i)\cdot S^+(m,j)] + S^z(n,i)\cdot S^z(m,j)\Big\} - \mu_0\sum_{n,i} g(n,i)\vec{H}\cdot\vec{S}(n,i) \tag{1}$$

with

$$J(N+n,i;N+m,j) = J(n,i;m,j), \tag{2}$$

where $N = N_A+N_B$, and n, m are the indices of the lattice planes, i and j are the sites in the atomic planes n and m, $g(n,i)$ and $\vec{H}$ are the Landé factor and the effective field, respectively. The interaction constants take the following values:

$$J(n,i;m,j) = \begin{cases} J_A \text{ for both sites in A,} \\ J_B \text{ for both sites in B,} \\ J_{AB} \text{ for one site in A and the other in B.} \end{cases} \tag{3}$$

The spin operators satisfy the following equation:

$$\hat{S}(n,i)\cdot\hat{S}(n,i) = S(n)[S(n)+1)] = \begin{cases} S_A(S_A+1) \text{ for sites in A,} \\ S_B(S_B+1) \text{ for sites in B.} \end{cases} \tag{4}$$

In terms of the discussion in references [19] and [26], the interface exchange constant $J_{AB} < 0$ will not destroy the ferromagnetic ground state in a biferromagnetic system if an external static field is applied to the system. Therefore, this theoretically allows the interface coupling to be less than zero. We consider two cases with $J(n,\, i;\, m,\, j) > 0$ and <0. The ground state of the system is all spin parallel. Using the method in reference [17], the Hamiltonian can be easily diagonalized and the eigenequations of the spin waves of the system can be obtained as follows:

$$\begin{aligned} E_{pk}f(n,p) = {} & [J(n,n)S(n) + J(n,n+1)S(n+1) \\ & + J(n,n-1)S(n-1) + \mu_0 g(n)H]\cdot f(n,k) \\ & - J(n,n+1)\sqrt{S(n)S(n+1)}f(n+1,k) \\ & - J(n,n-1)\sqrt{S(n)S(n-1)}f(n-1,k), \end{aligned} \tag{5}$$

with

$$f(n+N,p) = f(n,p), \tag{6}$$

where

$$\begin{aligned} J(n,n) &= 2(2-\cos k_x - \cos k_y)J(n,i;n,i\pm1) \equiv 2\gamma J_n, \\ J(n,n\pm1) &= J(n,i;n\pm1,i) = J(n\pm1,n). \end{aligned} \tag{7}$$

Here $E_{pk}(>0)$ is the excitation energy of the spin waves, $f(n,p)$ an orthonormalized wave function, which satisfy Born-Karman boundary condition. The index p in the wave functions is the wavevector of the spin waves parallel to the interface, and the parameter $\gamma = \gamma(\widehat{k}_{||}) = \gamma(k_x, k_y)$ defined by equation (7) varies from 0 to 4. We have chosen the lattice constants in both sublayers as unit length, i.e., the excitation energy and the wavevector of the spin waves mentioned in this paper are, respectively, the reduced excitation energy and the reduced wavevector.

Considering the periodic boundary condition, we assume the interfaces are formed between the planes $n = 1$, N and $n = N_A$, $N_A + 1$ for the present slabs. We will neglect the indices p, k of E_{pk} and p of $f(n,p)$ for simplicity, and set

$$f(n) = \begin{cases} f_A(n), \text{ for } 1 \leqslant n \leqslant N_A, \\ f_B(n), \text{ for } N_A+1 \leqslant n \leqslant N. \end{cases} \tag{8}$$

Due to the periodic boundary condition and the inversion symmetry in this system, the wave function $f(n)$ in the two sublayers may be written, respectively, as:

$$f_A(n) = \begin{cases} B_A^C \cos\left\{k_A[n-\frac{1}{2}(N_A+1)]\right\} & P=0, \\ B_A^S \sin\left\{k_A[n-\frac{1}{2}(N_A+1)]\right\} & P=1. \end{cases} \tag{9a}$$

$$f_B(n) = \begin{cases} B_B^C \cos\left\{k_B[n-N_A-\frac{1}{2}(N_B+1)]\right\} & P=0, \\ B_B^S \sin\left\{k_B[n-N_A-\frac{1}{2}(N_B+1)]\right\} & P=1, \end{cases} \tag{9b}$$

where B_i^j $(i = A, B; j = C, S)$ is a normalization constant, P represents the even parity $(P = 0)$ or the odd parity $(P = 1)$, k_A and k_B are, respectively, the wave-vector components perpendicular to the interfaces between the sublayers A and B. When k_A and k_B are both real, both complex (iq or $\pi \pm$ iq) (where $q > 0$), or one is real and the other is complex, we can obtain the bulk mode (BM), the interface mode (IM) and the perfect confined mode (PCM), respectively.

We define the interface-rescaling coefficient R as follows [22]:

$$\begin{aligned} f_B(N) &= Rf_A(1), \\ f_B(N_A+1) &= Rf_A(N_A). \end{aligned} \tag{10}$$

Inserting equation (10) into equation (5) and using the periodic boundary condition, one can obtain:

$$E = 2J_A S_A(1+\gamma-\cos k_A) + \mu_0 g_A H = 2J_B S_B(1+\gamma-\cos k_B) + \mu_0 g_B H, \quad (11)$$

and

$$\cot[\tfrac{1}{2}k_i(N_i+1)] = \frac{-\sin k_i}{\cos k_i - \mu_i^{-1}}\ P=0, \quad (12a)$$

$$\tan[\tfrac{1}{2}k_i(N_i+1)] = \frac{\sin k_i}{\cos k_i - \mu_i^{-1}}\ P=1, \quad (12b)$$

where the index i represents A or B, and the parameters μ_A and μ_B are given by:

$$\mu_A = 1 - \frac{J_{AB}S_B}{J_A S_A}(1-\alpha^{-1}R), \quad (13)$$

$$\mu_B = 1 - \frac{J_{AB}S_A}{J_B S_B}(1-\alpha R^{-1}), \quad (14)$$

where

$$\alpha = \sqrt{S_B/S_A}. \quad (15)$$

Solving equations (11) and (12), one can obtain k_A, k_B and R.

The ratio of coefficients B_B to B_A is determined by equation (10) and reduces to the normalization constants

$$\rho^C = B_B^C/B_A^C = R\cos[\tfrac{1}{2}k_A(N_A-1)]/\cos[\tfrac{1}{2}k_B(N_B-1)], \quad (16a)$$

$$\rho^S = B_B^S/B_A^S = -R\sin[\tfrac{1}{2}k_A(N_A-1)]/\sin[\tfrac{1}{2}k_B(N_B-1)]. \quad (16b)$$

Equation (11) shows that the excitation energy of the system has a simple translation when considering the Zeeman energy. So, in discussions below we assume the Zeeman energy is zero for the sake of simplicity.

3 The energy band fine structure of the 2D Brillouin zone

In this section, we analyze the energy band configuration of the longitudinal spin waves with varying transverse wave vector $\bar{k}_{||}$ along the high-symmetry directions of the 2D Brillouin zone (to see Fig. 1), and first give the fine structure of the energy band on the whole 2D Brillouin zone, that is to say, the evolvement curve of every branch of eigenmode on the 2D BZ. Without any loss of the generality we assume $J_A S_A > J_B S_B$ and choose the value of the parameter J_A, J_B, J_{AB}, S_A, S_B, N_A and N_B as, respectively, 1.0, 1/2, 2.0, 1, 1, 31 and 15.

We have calculated numerically the eigenproblems of the system corresponding to the above data. The numerical results show that the total number of spin-wave modes of the system is 46 ($=N_A+N_B$). For $\bar{k}_{||}=0$, the number of BMs is 30 in which there are 14 odd and 16 even parity modes. The number of PCMs in the sublayer A is 14, among which there are equal numbers of odd and even parity modes. The total number of IMs of the optic-optic type is 2 with different parities. All these results are similar to those in reference [22].

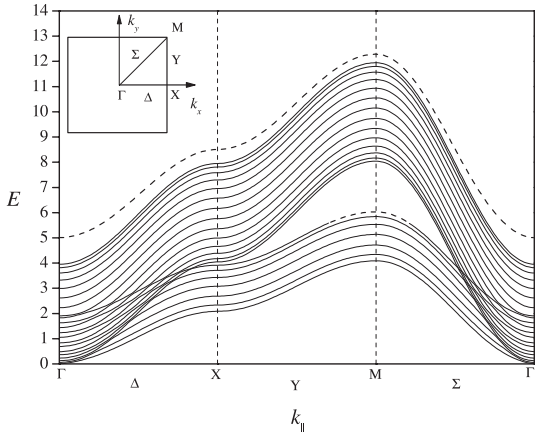

Fig. 1. The BZM of the magnetic bilayer corresponding to J_A, J_B, J_{AB}, S_A, S_B, N_A and N_B are, respectively, 1.0, 1/2, 2.0, 1, 1, 31 and 15: the higher energy band is subband A, the lower energy band is subband B, the highest dashed line denotes the optic-optic type IM and the dashed line inside the gap denotes the acoustic-optic type IM. Here, Edenotes the reduced excitation energy of the longitudinal spin waves, and $k_{||}$ denotes the reduced wavevector of the transversal spin waves. The 2D Brillouin zone of the bilayered system is plotted at the top left corner of the BZM, where Δ line, Y line and Σ line are three high-symmetry paths.

Only the energy band of the odd parity modes is plotted with varying $\bar{k}_{||}$ along the high-symmetry paths of 2D Brillouin zone in Figure 1 because that of the even parity modes is similar to the odd parity modes. The higher subband consists of PCMs in sublayer A, the lower subband is composed of PCMs in the sublayer B and the overlap of the subbands consists of BMs. The highest branch (dashed line) is IM of the optic-optic type, and the branch (dashed line segment) within the gap is IM of the acoustic-optic type. BMs are all standing waves that can freely propagate both in sublayers A and B. PCMs are standing waves in their own sublayer, while in the other sublayer they are interface decay waves that only can exist in the interface. IMs are interface decay waves in both sublayers. As the $\bar{k}_{||}$ value increases, seven branches of the higher energy BMs are transformed into the lower energy PCMs in sublayer A, while the other seven branches of BMs are transformed into the PCMs in sublayer B. As the $\bar{k}_{||}$ value sequentially increases, the highest branch of PCMs in sublayer B coming from BMs is transformed into the IM of the acoustic-optic type inside the gap.

Note that the IM of the acoustic-acoustic type cannot appear below both subbands, which is agreement with the results in references [21] and [25].

4 The conditions for the existence of ISW

In this section we will consider the conditions for the existence of acoustic-optic type and optic-optic type ISWs.

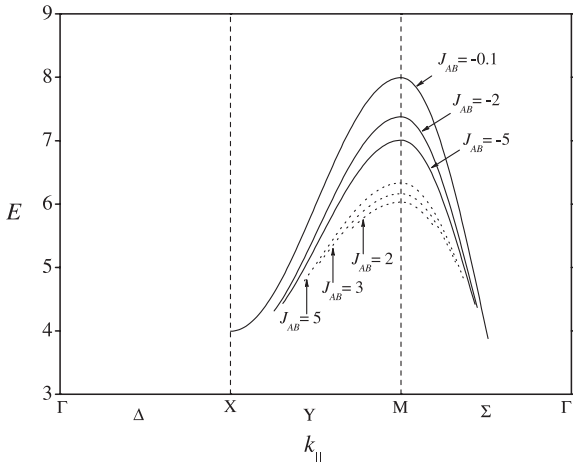

Fig. 2. The acoustic-optic type IMs over the 2D Brillouin zone corresponding to J_{AB}, respectively, equal to $-0.1, -2, -5, 5, 3$ and 2 from top to bottom. The solid lines denote IMs of $J_{AB} < 0$ and the dotted lines denote IMs of $J_{AB} > 0$. The other parameters are as for Figure 1.

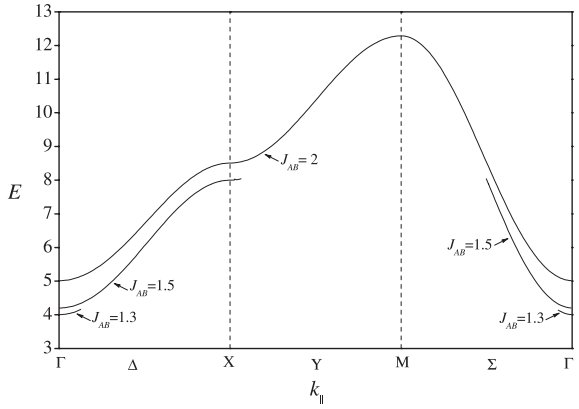

Fig. 3. The optic-optic type IMs of the 2D Brillouin zone corresponding to J_{AB} being, respectively, 2, 1.5 and 1.3 from top to bottom. The other parameters are as for Figure 1.

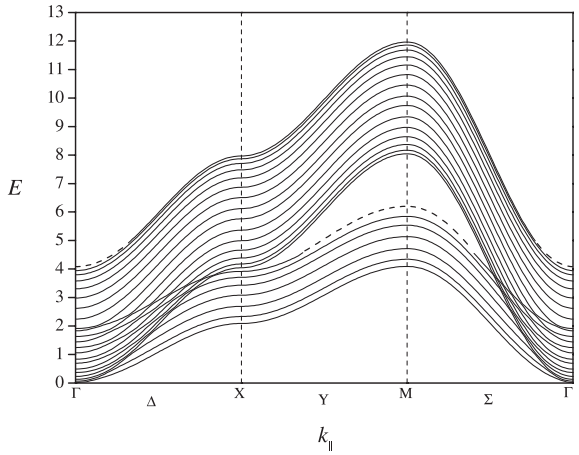

Fig. 4. The BZM of the magnetic bilayer corresponding to J_B and S_B, set to, respectively, 1.0 and 1/2, the other parameters are as for Figure 1. The highest dashed line denotes the optic-optic type IM and the dashed line inside the gap denotes the acoustic-optic type IM.

Firstly, the conditions for the existence are related to the interface exchange constant J_{AB}. For $J_{AB} > 0$, only when J_{AB} leads to strong ferromagnetic coupling can ISWs appear [21,25]. For $J_{AB} < 0$, ISWs also may appear in a semi-infinite symmetrical system of ferromagnetic bilayers [19]. On the condition of all parameters being the same as above, we find a branch of optic-optic type IMs appears when $J_{AB} > 1.27$ and it may exist over the whole Brillouin zone when $J_{AB} > 1.61$. Another branch of acoustic-optic type IMs also appears when $J_{AB} > 1.76$ in the finite asymmetrical system of ferromagnetic bilayers. But for $J_{AB} < 0$, no optic-optic type ISWs can appear while a branch of acoustic-optic type ISWs appears when $J_{AB} < -0.06$. In Figure 2, six branches of acoustic-optic type IMs are plotted corresponding, respectively, to $J_{AB} = -0.1, -2, -5, 5, 3$, and 2 from top to bottom. We find there is not the acoustic-optic type IM on the Δ region of 2D Brillouin zone. The acoustic-optic type IM (dotted lines) appears in the vicinity of the top of subband B when $J_{AB} > 0$, and it moves to the interior of the gap as J_{AB} increases. While the acoustic-optic type IM (solid lines) appears in the vicinity of the bottom of subband A when $J_{AB} < 0$, it also moves to the interior of the gap as $|J_{AB}|$ increases. This means the high energy subband easily attracts the antiferromagnetic interface coupling IM, and the low energy subband easily attracts the ferromagnetic interface coupling IM. When interface exchange coupling increases, the interface's attraction to IM increases too, so the IM moves to the interior of the gap. In Figure 3, three optic-optic type IM branches are plotted corresponding, respectively, to $J_{AB} = 2, 1.5$ and 1.3 from top to bottom. The results indicate that optic-optic type IM can only appear in the vicinity of the Γ point when J_{AB} is small, but may exist over the whole Brillouin zone when $J_{AB} > 1.61$. By the same reasoning as above, the IM moves away from subband A as J_{AB} increases.

Secondly, the conditions for existence are also related to the character of the magnetic layers A and B. For example, when the value of J_B is interchanged with that of S_B and the other parameters are kept unchanged, we find the BZM (see Fig. 4) is slightly different from that of Figure 1. The configurations of two subbands in Figures 1 and 4 are the same on the whole because $J_A S_A$ and $J_B S_B$ are unchanged. However, the optic-optic type IM (dashed lines above) appears in the vicinity of the Γ point on a 2D Brillouin zone. It is transformed into the PCM in sublayer A, and the region becomes large where the acoustic-optic type IM (dashed line within the gap) exists. Further study shows the optic-optic type IM appears when $J_{AB} > 1.90$ and it may exist over the whole Brillouin zone when $J_{AB} > 2.66$. The acoustic-optic IM appears when $J_{AB} > 1.30$ or $J_{AB} < -0.13$, and the IMs move away from the subbands as $|J_{AB}|$ increases. In addition, sublayer thickness N_A and N_B also influence IM. We do not discuss in further detail here.

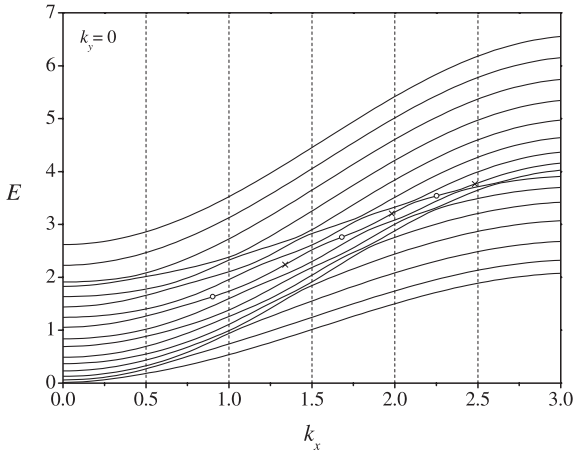

Fig. 5. Sixteen branches of the lower energy modes on the Δ region of 2D Brillouin zone. The line with circles and crosses denotes the 9th mode, which is the BM when $k_x \leqslant 2.520$ and is the PCM in the sublayer A when $k_x > 2.520$. Circles represent the resonance points in sublayer B and crosses represent the resonance points in sublayer A.

Finally, it is worth mentioning there are optic-optic type IMs and acoustic-optic type IMs in the even parity energy band, which are completely degenerate with those of the odd parity energy bands.

5 Resonant-confined spin waves in the bulk modes

In this section, we note that resonant-confined spin waves (RCSW) may exist in the bulk modes and the RCSWs may appear in both sublayers.

In Figure 1 (or Fig. 4), the variation of bulk modes with $\bar{k}_{||}$ is completely different from the perfect confined modes. In order to clearly show the difference, in Figure 5 we only plot 16 branches of the lower energy modes over the Δ region of the 2D Brillouin zone. The line labeled circles and crosses denotes the 9th eigenmode, which is the BM when $k_x \leqslant 2.520$ and is transformed into the PCM in the sublayer A when $k_x > 2.520$. The PCMs in A or B show cosine behavior with varying k_x, but the BMs do not have the clearly functional relation with k_x. BMs sometimes tend to the direction parallel to the subband A, and sometimes tend to the direction parallel to the subband B as k_x varies. When the frequencies of BMs are very close to the intrinsic frequencies of the sublayer material A (or B), RCSWs may appear. This kind of the spin wave is different from the extended bulk waves. Its amplitude is much higher in the corresponding sublayer than in that of the other sublayer. The spin waves of the 9th mode of the odd parity are plotted in Figure 6 corresponding, respectively, to $k_x = 0.451, 0.902$ and 1.339 over the Δ region of 2D Brillouin zone from (a) to (c). In the figure, f denotes the amplitude of the longitudinal spin waves, n denotes the number of atomic planes parallel to the interface, $n = 1$ to 31 is the sublayer A and $n = 32$ to 46 is the sublayer B. Figure 6a shows the extended bulk wave, whose amplitude is essentially the same in both sublayers. As k_x increases, the RCSW in sublayer B (see Fig. 6b) appears and the RCSW in sublayer A (see Fig. 6c) also appears with k_x sequentially increasing. Moreover, one can find oscillating behavior of RCSWs, that is to say, the RCSWs in sublayer A and B appear alternately as k_x increases. This is because the frequencies of BMs are sometimes very close to the intrinsic frequencies of the sublayer material A and sometimes very close to the intrinsic frequencies of the sublayer material B. For example, the resonance points in the sublayer B are represented in Figure 5 by circles for the 9th mode corresponding, respectively, to $k_x = 0.902, 1.681$, and 2.252, while those in the sublayer A are represented by crosses corresponding, respectively, to $k_x = 1.339, 1.982$ and 2.482. One can find circles alternate with crosses. There is the analogous phenomenon for the other BMs in this system.

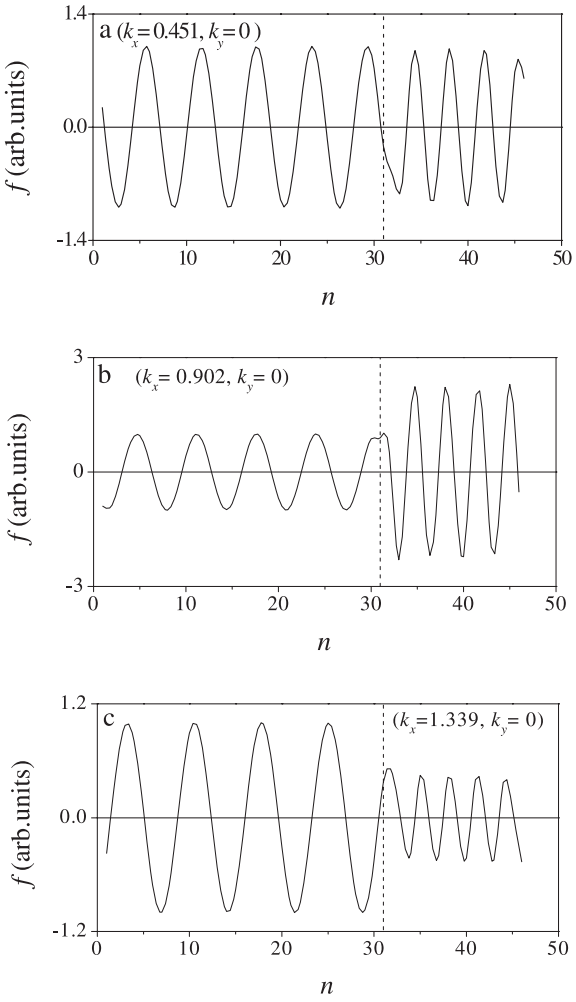

Fig. 6. The spin waves of the 9th mode of the odd parity corresponding, respectively, to $k_x = 0.451, 0.902$ and 1.339 from (a) to (c) in the Δ region of the 2D Brillouin zone. (a) Denotes the extended bulk wave; (b) and (c) denote the resonant-confined spin waves. Here f denotes the amplitude of the longitudinal spin waves, n denotes the number of the atomic planes parallel to the interface.

6 Conclusions

In conclusion, we find that there are three types of spin waves eigenmodes, namely, BMs, PCMs and IMs, in a general ferromagnetic bilayer system, which give the fine structure of the energy band over the whole 2D Brillouin zone. In BZM, either 0, 2 or 4 branches of IMs may exist, consisting of an equal number of odd and even parity modes which are completely degenerate. IMs are influenced by factors such as J_A, S_A, J_B, S_B, N_A, N_B and J_{AB}. As $|J_{AB}|$ increases, IMs move away from the subbands because they become strongly attracted to the interface. In BMs, RCSWs may exist when BMs tend to the direction parallel to the subband A or B and the RCSWs in the sublayer A alternate with those in the sublayer B as $\bar{k}_{||}$ varies.

This work was supported by NCET-2005, NSFC under Grant No. 10147203, the Key Project of Chinese Ministry of Education under Grant No. 206024 and Ph.D. Progress Foundation of higher education institutions of China under Grant No. 20040126003.

References

1. M.N. Baibich, J.M. Broto, A. Fert, F. Nguyen VanDau, F. Petroff, Phys. Rev. Lett. **61**, 2472 (1988)
2. R.E. Camley, R.L. Stamps, J. Phys.: Condens. Matter **5**, 3723 (1993)
3. D.J. Monsma, J.C. Lodder, Th.J.A. Popma, B. Dieny, Phys. Rev. Lett. **74**, 5260 (1995)
4. Ch. Tsang, R.E. Fontana, T. Lin, D.E. Heim, V.S. Speriosu, B.A. Gurney, M.L. Williams, IEEE Trans. Magn. **30**, 3081 (1994)
5. E.Y. Chen, S. Tehrani, T. Zhu, M. Durlam, H. Goronkin, J. Appl. Phys. **81**, 3992 (1997)
6. G.F. Hughes, IEEE Trans. Magn. **36**, 521 (2000)
7. C.T. Rettner, M.E. Best, B.D. Terris, IEEE Trans. Magn. **37**, 1649 (2001)
8. D. Smith, E. Chunsheng, S. Khizroev, D. Litvinov, J. Appl. Phys. **99**, 014503 (2006)
9. S. Maekawa, T. Shinjo, *Spin dependent transport in magnetic nanostructures* (Taylor, London and New York, 2002), Chap. 5
10. V. Novosad, M. Grimsditch, K.Yu. Guslienko, P. Vavassori, Y. Otani, S.D. Bader, Phys. Rev. B **66**, 052407 (2002)
11. J. Shibata, K. Shigeto, Y. Otani, Phys. Rev. B **67**, 224404 (2003)
12. K.Yu. Guslienko, S.O. Demokritov, B. Hillebrands, A.N. Slavin, Phys. Rev. B **66**, 132402 (2002)
13. M. Krawczyk, H. Puszkarski, J.C.S. Lévy, D. Mercier, J. Phys.: Condens. Matter **15**, 2449 (2003)
14. M.P. Kostylev, A.A. Stashkevich, N.A. Sergeeva, Phys. Rev. B **69**, 064408 (2004)
15. M. Bolte, G. Meier, C. Bayer, Phys. Rev. B **73**, 052406 (2006)
16. G. Leaf, H. Kaper, M. Yan, V. Novosad, P. Vavassori, R.E. Camley, M. Grimsdich, Phys. Rev. Lett. **96**, 017201 (2006)
17. H. Puszkarski, L. Dobrzynski, Phys. Rev. B **39**, 1819 (1989)
18. H. Puszkarski, Solid State Commun. **72**, 887 (1989)
19. H. Puszkarski, A. Akjouj, B. Djafari-Rouhani, L. Dobrzynski, Phys. Rev. B **51**, 16008 (1995)
20. H. Puszkarski, R. Jozefowicz, B. Kolodziejczak, A. Akjouj, B. Djafari-Rouhani, L. Dobrzynski, Surf. Sci. **352–354**, 914 (1996)
21. G.H. Yun, X.X. Liang, Eur. Phys. J. B **35**, 261 (2003)
22. G.H. Yun, J.H. Yan, S.L. Ban, X.X. Liang, Surf. Sci. **318**, 177 (1994)
23. X.X. Liang et al., *Theories of the Electron-Phonon Interaction and Spin-Waves in Layered Materials* (Inner Mongolia University Press, 1995), Chap. 5
24. W.P. Zhou, G.H. Yun, Surf. Sci. **553**, 75 (2004)
25. A. Yaniv, Phys. Rev. B **28**, 402 (1983)
26. H. Puszkarski, Surf. Sci. Rep. **20**, 45 (1994)
27. H. Puszkarski, S. Mamica, Horizons in World Physics **244**, 1 (2004)